Acta Chemica Scandinavica, 1994: 48: 960–966
Printed in Belgium – all rights reserved

ACTA
CHEMICA SCANDINAVICA
ISSN 0904–213X

Studies on the Gas-Phase Electron Diffraction Data of Tungsten Hexachloride and Lead Tetrachloride in View of Digital Fourier Filtering, Three-Atom Scattering and Accuracy of Scattering Functions

Tor G. Strand

Department of Chemistry, University of Oslo, PO Box 1033 Blindern, N-0315 Oslo, Norway

Strand, T. G., 1994. Studies on the Gas-Phase Electron Diffraction Data of Tungsten Hexachloride and Lead Tetrachloride in View of Digital Fourier Filtering, Three-Atom Scattering and Accuracy of Scattering Functions. – Acta Chem. Scand. 48: 960–966 © Acta Chemica Scandinavica 1994.

The gas-phase electron diffraction data of the respectively octahedral and tetrahedral molecules tungsten hexachloride and lead tetrachloride have been reinvestigated by adding three-atom scattering, computed according to an approximate expression, to the calculated intensities. Relatively large contributions, which lead to a considerably better agreement with the data, are computed for tungsten hexachloride. This increases the W–Cl distances by the formally significant amount of 0.008(2) Å and reduces the W–Cl vibrational amplitudes from 0.078(2) to 0.053(1) Å. A smaller contribution calculated for lead tetrachloride improves the agreement noticeably, with no significant changes in the structure parameters. Experimental corrections to the heavy-atom–chlorine scattering functions computed as five-term polynomials indicate that the standard tabulated scattering factors of the heavy atoms are not very accurate. Fourier filtering of the photometer data improve the reproducibility of the data as well as the least-squares agreement with the models. A new variant of the autocorrelation power spectrum with a higher resolution in the distance domain than the traditional radial distribution function is explained and illustrated.

In the investigations of several heavy central atom inorganic or metalorganic compounds carried out by the Oslo electron diffraction group, the vibrational amplitudes of the molecules often turn out larger than expected. Improved agreement with the data is frequently obtained by the multiplication of the phases of the complex atomic scattering factor of the heavy atom by some factor. This has led to a growing suspicion about the accuracy of the standard tabulated scattering factors of heavier atoms. Two examples are the binary chlorine compounds tungsten hexachloride[1] and lead tetrachloride.[2] In the octahedral tungsten hexachloride improved agreement was obtained by multiplication of the phases of the scattered amplitudes of the tungsten atom by the factor 1.07; reasonable agreement was then obtained between the calculated and experimental vibrational amplitudes. For the tetrahedral lead tetrachloride, a smaller factor of 1.03 was applied; however, the experimental Pb–Cl vibrational amplitude was determined to be 0.058(2) Å, which is considerably larger than the value calculated from spectroscopic data of 0.049 Å. In tungsten hexachloride, some contribution from three-atom scattering, which was not included in the previous investigations, would be expected. Thus, it seemed of interest to reanalyze the data of these two molecules to see if three-atom scattering could explain at least part of the observed discrepancies.

The photometer data of the Oslo group have for a long period been digitally Fourier-filtered; this process is described and discussed. A new variant of the autocorrelation power spectrum is explained and illustrated. For the two highly symmetrical molecules, the resolution of this spectrum in the *r*-domain is sharper than the resolution of the radial distribution function.

Fourier filtering and data reduction

Optical densities recorded by our Snoopy microdensitometer for the previous investigations[1,2] were employed. Snoopy oscillates the plates about 11° around the center of the in theory radial symmetric scattering pattern. The light quanta transmitted through one oscillation are counted for each step of 0.1 mm. Coarse errors are removed by visual inspection of the data. The data were from six plates for both a long (about 50 cm) and for a

short (about 25 cm) camera distance. The s ranges and intervals applied for the average molecular intensities were 1.875, 14.500, 0.125 and 4.00, 28.00, 0.25 Å^{-1} for both molecules.

The photometer data from the Oslo electron diffraction group are routinely filtered by a digital Fourier filter.[3] The molecular intensities are periodic functions according to

$$\sin(r_a s) = \sin\left[2\pi r_a\left(\frac{s}{2\pi}\right)\right] \Leftrightarrow \sin(2\pi f t) \qquad (1)$$

With $s/2\pi$ as the independent variable, $s/2\pi$ and r_a obviously correspond to the traditionally denoted time (t) and frequency (f) domains of periodic functions. The applied equidistant s intervals of 0.125 and 0.25 Å^{-1} have Nyquist critical frequencies of 25.1 and 12.6 Å. The corresponding Nyquist frequencies of the photometer data for the step size of 0.1 mm estimated by eqn. (3) of Ref. 3 are about 147 and 74 Å. In the transformation from the photometer- to the s scale, frequencies of the photometer data in between the two limiting frequencies would alias into the narrower frequency range of the s scale. To avoid this aliasing, the cut frequencies of the filters were set to the Nyquist frequencies of the applied s intervals, assuming that this way to smooth the photometer data would minimize the expected increase of the correlation in the relative intensities on the s scale.

The original center of the plate was adjusted by demanding that the first derivatives of each side should be as equal as possible. The photometer data for each side of the plates were transferred to the s scale by linear interpolations, a single hit blackness correction with $d = 0.35$ was applied[4] and the relative intensities were obtained by corrections for the rotating sector[5] and the application of planar plates. Levelled intensities were obtained by division with the background computed from the applied atomic scattering factors[6] and scaled to an average value of one.

Backgrounds were drawn on the levelled intensities from each side of the plates as fifth- (long camera distance data) and sixth- (short camera distance data) degree polynomials to the differences between experimental and calculated intensities by the least-squares method. The molecular intensities for each side of the plates were scaled to an average background value of one and were based on the modification function $s/|f'(s)_{Cl}|^2$. The average molecular intensities with standard deviations, regarding the data from one plate as one observation, were computed. The calculated intensities are scaled in the least-squares refinements to the average experimental ones for both of the camera distances, and for perfect agreement between experiment and model, these least-squares scale factors should be equal to one for the levelled experimental intensities scaled to an average background value of one.[7] In practice, values of the scale factors somewhat smaller than one are determined; these scale factors are equivalent to Bartell's indices of resolution[8] and give a measure of the agreement between the experimental data and the applied model. In addition the unweighted and weighted percentage factors R_u and R_w are extensively used to judge the agreement between two related data sets $I_{1,i}$ and $I_{2,i}$:

Table 1. Comparision of the average percentage R-factors R_u and R_w obtained for the molecular experimental intensities from each side of the plates in relation to the total average experimental intensities for the unfiltered and digitally Fourier filtered data of the two camera distances.

	WCl_6		$PbCl_4$	
Camera distance	Long	Short	Long	Short
R_u, unfiltered:	4.6	18.8	8.8	23.8
R_u, filtered:	3.1	13.3	6.6	16.8
R_w, unfiltered:	3.8	12.3	7.6	15.7
R_w, filtered:	2.4	7.8	5.9	10.6

$$R_u = 100\frac{\sum|I_{1,i} - I_{2,i}|}{\sum|I_{2,i}|} \qquad (2)$$

$$R_w = 100\left(\frac{\sum[w_i(I_{1,i} - I_{2,i})]^2}{\sum w_i I_{2,i}^2}\right)^{1/2}, \quad w_i = \frac{1}{\sigma_i^2} \qquad (3)$$

The R_u and R_w values for the molecular intensities of each side of the plates measured against the average molecular intensities of all the plates were calculated for both the unfiltered and the digitally Fourier filtered photometer data. The averages of these R factors are given in Table 1. Smaller factors should indicate a higher

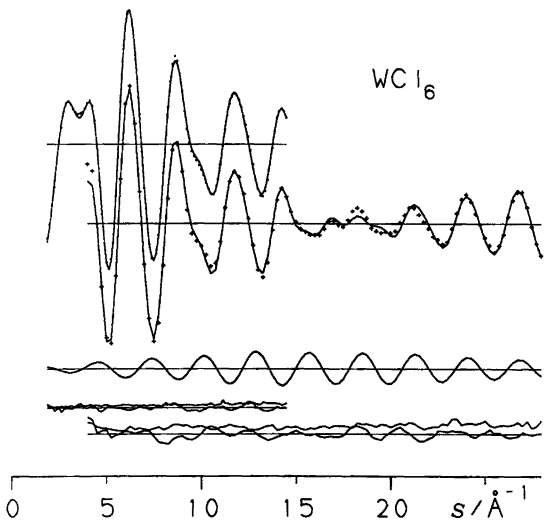

Fig. 1. Tungsten hexachloride. Above: experimental (+) and calculated (−) molecular intensities of the long and short camera distance data. Below: calculated three-atom scattered intensities and the differences between the experimental and calculated intensities with standard deviations of the average experimental intensities.

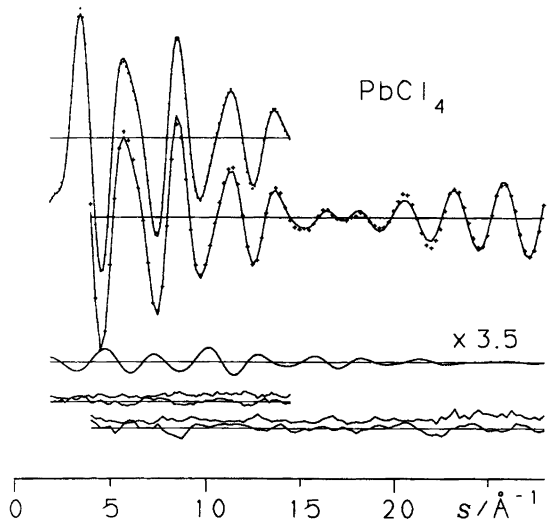

Fig. 2. Lead tetrachloride. Above: experimental (+) and calculated (−) molecular intensities of the long and short camera distance data. Centre: calculated three-atom scattered intensities multiplied by the factor 3.5, which is the ratio of the total number of $l_{ij,k}$ terms of $PbCl_4$ and WCl_6. Below: differences between the experimental and calculated intensities with standard deviations of the average experimental intensities.

internal consistency of the data set. The average molecular intensities and standard deviations obtained for the two molecules are included in Figs. 1 and 2.

Three-atom scattering. In the three-atom scattering, a wave from an atom i enters an atom j and the outgoing wave from j interferes with an outgoing wave from a third atom k. Accordingly, three-atom scattered intensities involve the sum over all triangles in the molecule. A first application of the Glauber approach to three-atom scattering gave a simple expression[9] which accounted for the discrepancies between the observed and the conventionally calculated molecular intensities of rhenium hexafluoride.[10] A correction to the orientational averaging procedure used in Ref. 9 has been discussed,[11] and this expression seemed to work well for tellurium hexafluoride.[12] The shadow propagation model introduced a phase factor to take care of the three-dimensional structure of the molecule,[13] and the orientational average was modified to incorporate the shadow propagation model.[14] The simplest of these expressions for contributions from three-atom scattering is the shadow propagation model according to eqn. (23) of Ref. 13, and the present calculations were started from this expression. The calculated three-atom scattered contributions for tungsten hexachloride showed improved agreement with the data by including the correction term ε of eqn. (32) of Ref. 11 in the argument of the Bessel function. This term is proportional to $1/r_{ij}^2$ and further connected to the first and second derivatives of the scattering factors with respect to s_i and s_j. Including the effects of molecular vibrations,[11] the equation used to compute the three-atom intensities was

$$I_{ij,k}(s) = -\frac{2}{kr_{ij}^2} J_0\left[sr_k\left(1 - \varepsilon - \frac{1}{2}\omega^2\right)\right]$$
$$\times |f_i(s_i)||f_j(s_j)||f_k(s)|(1 - \varepsilon l_{\parallel}^2 s^2)\, e^{-l_{\perp}^2 s^2/2}$$
$$\times \sin\left[\eta_i(s_i) + \eta_j(s_j) - \eta_k(s) + \left(\frac{r_{ij}}{2k}\right)(ss_i - s_i^2)\right] \qquad (4)$$

where

$$\omega^2 = l_{\parallel}^2/r_k^2 \qquad (5)$$

r_k is the projection from atom k to the connection line between atoms i and j. $l_{\perp}$ and $l_{\parallel}$ are the components of the root mean-square vibrational amplitudes perpendicular and parallel to r_{ij} relative to the intersection of the normal from k to r_{ij}. For a more precise definition of the different symbols, the reader is referred to the articles cited. The three-atom intensities computed in this way are included in Figs. 1 and 2 and the contributions to the radial distribution functions are shown in Figs. 3 and 4. For the short camera distance data of tungsten hexachloride, the absolute values of the computed three-atom scattered intensities are 29% of the absolute values of the total computed molecular intensities. In lead tetrachloride this percentage is reduced to 4%, and in Fig. 2 the computed three-atom scattered intensities for lead

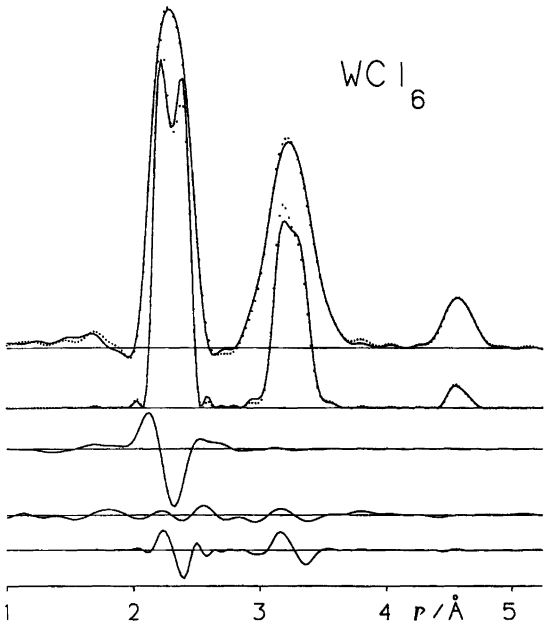

Fig. 3. Tungsten hexachloride. Above: experimental (•) and calculated (—) radial distribution functions and autocorrelation power spectra. Below: Fourier sine transform of the calculated three-atom scattered intensities and differences between the experimental and the calculated radial distribution functions and power spectra.

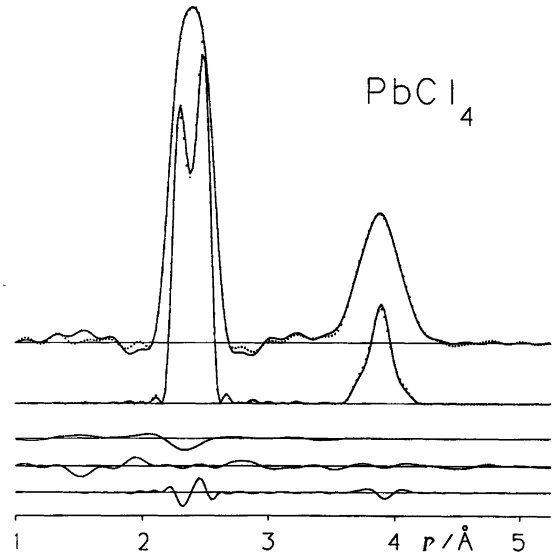

Fig. 4. Lead tetrachloride. Above: experimental (•) and calculated (–) radial distribution functions and autocorrelation power spectra. Below: Fourier sine transform of the calculated three-atom scattered intensities and differences between the experimental and the calculated radial distribution functions and power spectra.

tetrachloride were multiplied by the factor 3.5, which is the ratio between the total number of *ij,k* terms of the two molecules. The dominant effect of the molecular vibrations on the three-atom scattered intensities is the exponential term in eqn. (4). As demonstrated in Figs. 1 and 2, the three-atom scattered intensities calculated for the right-angled triangles of tungsten hexachloride are the less dampened,[13] and for this molecule an $l_\perp$ value in the range 0.05–0.06 Å gave the best agreement with the experimental data. This range is consistent with the vibrational amplitude of the W–Cl distance computed from spectroscopic data.[1] The vibrational parameters of the three-atom intensities were estimated from the vibrational amplitudes calculated from spectroscopic data;[1,2] however, for non-right-angled triangles the three-atom scattered intensities fall off so rapidly that an accurate estimate of the vibrational parameters does not seem to be critical.

Calculation of a correction to the scattering functions

For the chosen modification function of $s/|f'_{Cl}(s)|^2$ the scattering function $g(s)$ of the molecular intensities[15] for the Cl···Cl distances is equal to one, and for harmonic vibrations these peaks on the radial distribution function should have a gaussian shape. The scattering functions of the X–Cl distances of the molecules are then

$$g^{calc}_{X-Cl}(s) = \frac{|f_X(s)|}{|f_{Cl}(s)|}\cos[\eta_x(s) - \eta_{Cl}(s)], \quad X = W, Pb \qquad (6)$$

Including the calculated three-atom scattered intensities in the least-squares refinements, most of an asymmetric difference between the experimental and calculated W–Cl peaks of the radial distribution function of tungsten hexachloride was removed. For both of the molecules the difference was now approximately symmetric about the X–Cl distance and sufficiently large to indicate a systematic error in the computed $g_{X-Cl}(s)$ functions. The differences between the experimental and calculated Cl···Cl peak(s) were considerably smaller. The calculation of an experimental correction to the scattering functions, $\Delta g_{X-Cl}(s)$, from the experimental intensities and the least-squares model is straight forward; the experimental intensities are scaled to the theoretical ones, connected and brought on the same s intervals of 0.25 Å^{-1} and averaged for part of the overlap region. Then three-atom intensities and Cl···Cl contribution(s) are subtracted, the resulting X–Cl contribution is antidampened, and divided by $\sin(r_{a,X-Cl}s)$ and the multiplicity of this distance, which leaves an experimental $g_{X-Cl}(s)$ including all systematic and experimental errors. Finally, a correction is obtained by subtracting the computed $g_{X-Cl}(s)$. On the assumption that this correction should be smooth and with a relatively long period, N-term polynomials were fitted to the experimental correction by the least-squares method applying the singular value decomposition method.[16] Before the least-squares refinements were carried out, some large corrections, arising from the division with small values of $\sin(r_{a,X-Cl}s)$, were set equal to zero, and the standard deviations for the weights in the least-squares calculations were set proportional to the inverse of the absolute value of this sine function. A five-term polynomial was necessary, and this polynomial worked better than a six-term one. According to this scheme

$$g^{ex}_{X-Cl}(s) = g^{calc}_{X-Cl}(s) + \Delta g^{ex}_{X-Cl}(s)$$
$$= g^{calc}_{X-Cl}(s) + \sum_{i=0}^{4} a_i s^i. \qquad (7)$$

The scattering functions computed from the tabulated values[6] and the experimental correction terms are

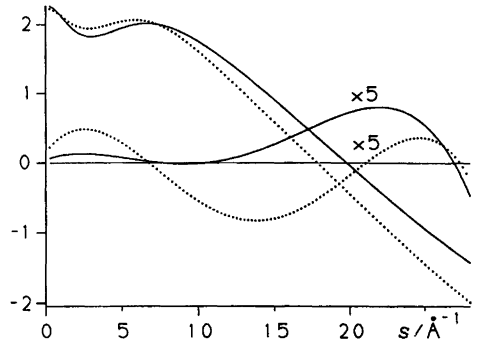

Fig. 5. Calculated scattering functions according to eqn. (6) and the experimental correction terms of eqn. (7) multiplied by a factor of five for WCl_6 (–) and $PbCl_4$ (•).

Table 2. The constants a_i for the five-term polynomials of the correction terms to the W–Cl and the Pb–Cl scattering functions according to eqn. (7).

Constant a_i	W–Cl	Pb–Cl
a_0	0.9451×10^{-2}	0.3124×10^{-1}
a_1/Å	0.1637×10^{-1}	0.5762×10^{-1}
a_2/Å^2	-0.4765×10^{-2}	-0.1465×10^{-1}
a_3/Å^3	0.3890×10^{-3}	0.9153×10^{-3}
a_4/Å^4	-0.8730×10^{-5}	-0.1676×10^{-4}

illustrated in Fig. 5. In Table 2 the values of a_i for the five-term polynomials of the correction terms are given.

Least-squares refinements

The structure parameters, r_a distances and root mean-square vibrational amplitudes l, were determined by the Levenberg–Marquardt method for nonlinear least-squares by the application of FORTRAN subroutines of Ref. 16. The distances were refined independently of geometrical models, however, with proper multiplicities according to the known molecular symmetries. The calculated intensities were scaled to the experimental ones by one scale factor for the data from each of the two camera distances. This gives altogether eight parameters to be refined for tungsten hexachloride and six for lead tetrachloride. The standard deviation computed for the average molecular intensities was applied for the diagonal weighting matrix. The best results are regarded as those where the three-atom scattered intensities were included in the calculated ones and where the calculated intensities were based on the experimentally corrected scattering functions. The results are given in Tables 3 and 4. The standard deviations of these two tables are uncorrected least-squares values which should be doubled to take care of correlated data, and the standard deviations of the distances should be expanded by 0.1% to include an estimated uncertainty of the scale. In Table 5 the agreement

Table 3. Least-squares results for tungsten hexachloride with three-atom scattered intensities included and based on the experimentally corrected scattering function of the W–Cl distance.[a]

	Least-squares values	Force field values[1]
r_a(W–Cl)	2.2893(5)	
l(W–Cl)	0.0528(12)	0.056
r_a(Cl···Cl)$_{90}$	3.2253(10)	
l(Cl···Cl)$_{90}$	0.1463(11)	0.140
r_a(Cl···Cl)$_{180}$	4.5574(37)	
l(Cl···Cl)$_{180}$	0.0855(46)	0.074
δ(Cl···Cl)$_{90}$	0.0123(12)	0.005
δ(Cl···Cl)$_{180}$	0.0212(38)	0.008

[a] r_a distances, root-mean square vibrational amplitudes l and shrinkage δ based on the r_a geometry. The uncorrected least-squares standard deviations times 10^4 are given in parenthesis. All the parameters are in Å units.

Table 4. Least-squares results for lead tetrachloride with three-atom scattered intensities included and based on the experimentally corrected scattering function of the Pb–Cl distance.[a]

	Least-squares values	Force-field values[2]
r_a(Pb–Cl)	2.3693(6)	
l(Pb–Cl)	0.0482(13)	0.049
r_a(Cl···Cl)	3.8643(20)	
l(Cl···Cl)	0.1406(18)	0.139
δ(Cl···Cl)	0.0048(21)	0.010

[a] r_a distances, root-mean square vibrational amplitudes l and shrinkage δ based on the r_a geometry. The uncorrected least-squares standard deviations $\times10^4$ are given in parenthesis. All the parameters are in Å.

Table 5. Least-squares scale factors (index of resolution) k and percentage unweighted R-factors R_u for the data from the two camera distances of the molecules.[a]

	WCl_6				$PbCl_4$			
	Long		Short		Long		Short	
	k	R_u	k	R_u	k	R_u	k	R_u
a	0.948	5.2	0.933	24.9	0.939	5.6	0.934	17.0
b	0.963	3.9	0.946	12.9	0.962	5.3	0.958	14.9
c	0.955	3.5	0.942	11.8	0.931	4.3	0.929	10.6
d	0.950	4.8	0.922	12.8	0.925	4.4	0.918	12.6

[a] From above: (a) Fourier-filtered data, scattering functions from tabulated scattering factors and three-atom scattering not included. (b) As for (a) except that three-atom scattering is included. (c) includes in addition to three-atom scattering use of the experimentally corrected scattering functions of the heavy atoms. (d) is identical to (c) exept that it is based on unfiltered data.

expressed by k and R_u is shown for refinements of all the parameters; (a) with the g(X–Cl) values from tabulated scattering factors and no three-atom scattered intensities included, (b) with three-atom intensities included and (c) using the experimentally corrected g(X–Cl) values in addition to include the three-atom scattering. Thus (c) gives the agreement for the parameters of Tables 3 and 4. Important changes of the structure parameters through the steps (a)–(d) are discussed later in the paper. The radial distribution functions of Figs. 3 and 4 were computed by the fast discrete Fourier sine transform (SINFT of Ref. 16) by scaling the experimental intensities according to the least-squares results, transforming to the common s interval of 0.25 Å^{-1}, averaging for part of the overlap region and adding the inner calculated intensities. A dampening function of $\exp(-0.0025s^2)$ was applied to the intensities before the discrete transform, and the intensities were zero-padded to $2^9 = 512$ points, which gives an r interval of 0.0245 Å. The R_u values for the plotted range of the radial distribution functions were 4.9% for tungsten hexachloride and 5.1% for lead tetrachloride.

An autocorrelation power spectrum

Use of the autocorrelation power spectrum as a representation of the molecular intensities in the r domain has been investigated.[17] The autocorrelation process transfers dampened sine functions to still more dampened cosines in the s domain, and the r representation is acquired by a Fourier cosine transform. The extra dampening of the autocorrelation function may be canceled by a weighting function. An important property of the autocorrelation function, which was noticed in Ref. 17, is that the autocorrelation may be started at any s value: the sines are still properly transferred to cosines. The new variant is to invert the intensities through $s = 0$, which conserves the periodicity of the sines as the sine function is an uneven function. This function of doubled s range from $-s_{max}$ to s_{max} gives an autocorrelation function from 0 to about $2s_{max}$. Theoretical intensities are added to the experimental ones from $s = 0$ to s_{min} before inversion through the origin. The power spectrum of this function is calculated by the fast discrete Fourier cosine transform.

The autocorrelation power spectra of the two molecules computed in this way are included in Figs. 3 and 4. The autocorrelation was calculated by the FORTRAN subroutine CORREL,[16] and the Fourier cosine transform was carried out by COSFT,[16] both routines using the fast discrete Fourier transform. The intensities may be weighted by some function before the inversion through the origin; however, for the s range of the present data, the dampening inherent in the present autocorrelation process seems close to the optimal one. The heights of the peaks at higher r values are more reduced in the power spectrum than in the radial distribution function. To cancel this effect partly, the spectra of the r range shown in Figs. 3 and 4 were linearly increased by a factor from 1 at r_{min} to 10 at r_{max}.

The resolution of the spectra shown in Figs. 3 and 4 is sharper than the resolution of the corresponding radial distribution functions. On the autocorrelation power spectra the splits of the X–Cl peaks due to the phase shift of $\pi/2$ and more in the scattering functions (Fig. 5) are resolved. The differences between the experimental and calculated spectra seem to have about the same shape as, but to be somewhat larger than, the radial distribution function differences. Further investigations of the properties of this autocorrelation power spectrum as an aid in the solution of more complicated molecular structures seem of interest.

Results and discussion

Three-atom scattering and the corrected scattering functions. Three structure parameters are significantly changed through these two steps. The W–Cl distance is elongated and the W–Cl vibrational amplitude is reduced by including three-atom scattering. The Pb–Cl amplitude is reduced by application of the corrected g function.

By adding the computed three-atom scattered intensities to the theoretical ones for tungsten hexachloride, the agreement with the experimental data is considerably improved, as may be seen by comparing the k and R_u values of lines (a) and (b) in Table 5. The W–Cl distance increases from 2.2814(7) [2.281(3) in Ref. 1] to 2.2893(5) Å. Doubling both of the standard deviations to take care of data correlation, the difference of 0.0079(17) Å is formally significant.

The W–Cl vibrational amplitude obtained in the previous work[1] by multiplication of the phase shift of the W scattering factor by about 1.07 was 0.058(3) Å. The value obtained applying the tabulated scattering factors was 0.0782(19) Å, which by inclusion of three-atom scattering was reduced to 0.0531(13) Å.

The much smaller amount of three-atom scattering computed for lead tetrachloride still leads to a noticeably improved agreement with the data [Table 5, lines (a) and (b)]. The Pb–Cl distance of 2.3693(6) Å agrees with the value of 2.373(3) Å of Ref. 2, and the vibrational Pb–Cl amplitude obtained in this investigation by the multiplication of the phase shift of the Pb scattering factor by about 1.03 was 0.058(2) Å. A value of 0.0602(16) Å was obtained by the application of the tabulated scattering factors. None of the structure parameters of this molecule was essentially changed by the inclusion of the three-atom scattering.

Employing the experimentally corrected scattering functions for the X–Cl distances in addition to the inclusion of the three-atom scattering, the parameters of Table 5 (b) and (c) show that all the R_u values are further reduced; however, so are also all the k values. The main change of the structure parameters is the reduction of the Pb–Cl vibrational amplitude from 0.0602(16) to 0.0482(13) Å, a value in better agreement with the amplitude computed from spectroscopic data of 0.049 Å.[2] The W–Cl amplitude is only slightly reduced from 0.0531(13) to 0.0528(12) Å (0.056 Å from spectroscopic data[1]).

Thus improved agreement with the spectroscopically estimated W–Cl vibrational amplitude and with the data is obtained by including the three-atom scattering according to the expression (5) in the calculated intensities. This expression is an approximation, and a better estimate might of course lead to further improvements. The formally significant elongation of the W–Cl distance might be sensible to minor errors in the periodicity of the Bessel function, and it should be mentioned that this elongation leads to a poorer agreement with the spectroscopically computed shrinkage values (Table 3) than was obtained in Ref. 1. In the case of lead tetrachloride it seems unlikely that an improvement in the calculated three-atom intensities could be sufficiently large to take care of the indicated errors in the Pb–Cl scattering function. The accuracy of the experimentally determined corrections were limited by the shape of the applied polynomial as well as errors of the data, and a high precision cannot be expected. One may at least hope that they give some

Table 6. Average correlation coefficients ρ as function of $|s_k - s_l|$ in $Å^{-1}$ for unfiltered (U) and filtered (F) data of the long and short camera distance data of the molecules.

	WCl_6				$PbCl_4$			
	Long		Short		Long		Short	
$\|s_k - S_l\|$	U	F	U	F	U	F	U	F
0.125	0.46	0.56			0.72	0.78		
0.250	0.31	0.33	0.37	0.56	0.53	0.56	0.41	0.59
0.375	0.17	0.15			0.35	0.34		
0.500	0.08	0.03	0.13	0.27	0.16	0.15	0.19	0.39
0.750	−0.07	−0.04	−0.03	0.09	−0.14	−0.13	0.00	0.15
1.000	−0.25	−0.19	−0.08	0.02	−0.36	−0.33	−0.13	0.01

indication of the size and form of the errors, which were also demonstrated by the incorrect phase shifts observed in previous studies. The suspicion about the accuracy of the scattering factors of heavy atoms in this range does not seem to be lessened by the present results. Improved calculations seem desirable, if possible.

Digital Fourier filtering. The different *R* factors of Table 1 show an improved agreement from 22 to 37% for the Fourier-filtered photometer data. In the least-squares refinements the improvements of the R_u values vary from 2 to 27% [Table 5, lines (d) and (c)]. None of the structure parameters was significantly changed by the filtering. Setting the cut frequencies of the filter to the Nyquist limiting frequencies of the applied *s* intervals, the idea was not to achieve aliasing of these high frequencies of the photometer data into the intensities on the *s* scale, in this way hoping to minimize an expected rise of data correlation by the smoothing. The average correlation coefficients[18] $\rho(|s_k - s_l|)$ are compared in Table 6 for the filtered and unfiltered data. For the long camera distance the data correlation rises moderately owing to the filtering process, while the larger increase of the short camera distance data correlation is somewhat worrisome and indicates that a higher cut frequency might be tried to see if the correlation of the filtered data could be reduced.

The close to one hundred points on *s* scale finally used for the data from both camera distances are, for the applied photometer step of 0.1 mm, based on nearly 585 photometered points. The filtered photometer data are a function of all these points, and the reason for the higher Nyquist limiting frequency of the photometer data is of course this larger number of points. With the same number of points of the two scales, the presented way to filter would not allow the use of any filtering process. Thus this filtering is not a mere cosmetic smoothing of the data, but a way to include more of the information of the plates into the structure analysis.

References

1. Haaland, A., Martinsen, K.-G. and Shlykov, S. *Acta Chem. Scand. 46* (1992) 1208.
2. Haaland, A., Hammel, A., Martinsen, K.-G., Tremmel, J. and Volden, H. V. *J. Chem. Soc., Dalton Trans.* (1992) 2209.
3. Kjeldseth Moe, O. E. and Strand, T. G. *J. Mol. Struct. 128* (1985) 13.
4. Gundersen, S., Strand, T. G. and Volden, H. V. *J. Appl. Crystallogr. 25* (1992) 409.
5. Almenningen, A., Strand, T. G. and Volden, H. V. *The Norwegian Electron Diffraction Group, Annual Report* (1988) 14.
6. Ross, A. W., Fink, M. and Hilderbrandt, R. *International Tables for Crystallography*, Kluwer Academic Publishers, Dordrecht 1992, Vol. C, p. 245.
7. Strand, T. G. *J. Chem. Phys. 44* (1966) 1611.
8. Bonham, R. A. and Bartell, L. S. *J. Chem. Phys. 31* (1959) 702.
9. Bartell, L. S. and Wong, T. W. *J. Chem. Phys. 56* (1972) 2364.
10. Jacob, E. J. and Bartell, L. S. *J. Chem. Phys. 53* (1970) 2231.
11. Wong, T. C. and Bartell, L. S. *J. Chem. Phys. 58* (1973) 5654.
12. Gundersen, G., Hedberg, K. and Strand, T. G. *J. Chem. Phys. 68* (1978) 3548.
13. Bartell, L. S. *J. Chem. Phys. 63* (1975) 3750.
14. Miller, B. R. and Bartell, L. S. *J. Chem. Phys. 72* (1980) 800.
15. Andersen, B., Seip, H. M., Strand, T. G. and Stølevik, R. *Acta Chem. Scand. 23* (1969) 3224.
16. Press, W. H., Flannery, B. P., Teukolsky, S. A. and Vetterling, W. T. *Numerical Recipes*, Cambridge University Press, Cambridge 1986.
17. Trætteberg, M. and Bonham, R. A. *J. Chem. Phys. 42* (1965) 587.
18. Seip, H. M., Strand, T. G. and Stølevik, R. *Chem. Phys. Lett. 3* (1969) 617.

Received March 11, 1994.